P1.3

SURFACE-BASED INFRARED INTERFEROMETERS – VERSATILE SENSORS FOR THE IPY

Peter J Minnett,* Malgorzata Szczodrak and Erica L. Key
University of Miami, Miami, Florida

1 INTRODUCTION

Calibrated Fourier-Transform Infrared (FTIR) spectroradiometers have been used successfully in Polar Regions for several years in several settings, including ship-based expeditions into the Arctic and on a tower over the icecap in Antarctica. In addition the Atmospheric Radiation Measurement Program (ARM; Stokes and Schwartz, 1994) has deployed an Atmospheric Emitted Radiance Interferometer (AERI) as the North Slope of Alaska site for several years (Stamnes et al., 1999). The ship-based measurements have been made using Marine-AERIs (M-AERIs; Minnett et al., 2001) and the Antarctic data using a Polar-AERI (Walden et al., 2005; this symposium).

M-AERIs have been deployed on several icebreaking research vessels (USCGC *Polar Sea,* USCGC *Polar Star,* NCGC *Pierre Radisson,* NCGC *Amundsen* and RSV *Aurora Australis*) in both the Arctic and Antarctic (Figure 1). The M-AERI measurements have been analyzed to retrieve skin surface temperatures, spectral emissivity of the surface, near surface air temperatures, and profiles of atmospheric temperature and humidity to a height of about 3 km above the ship. In other experiments at lower latitudes, the M-AERI spectra of atmospheric emission have been analyses to determine the infrared radiative forcing of aerosols (Vogelmann et al., 2003).

The use of ship-based remote sensing in the Arctic has many advantages, especially when the ice cover is breaking up and installation of in situ sensors is impractical. The measurements can be conducted over long periods without special considerations for dedicated deployments of platforms (e.g. Ice-Raids or Ice Camps). Another important application of FTIR spectra and the derived geophysical variables is in the refinement of algorithms used with satellite measurements and validating the retrieved variables. FTIRs with proven track-records on the Polar environments can make important contributions to IPY projects.

2 THE M-AERI

The M-AERI is a seagoing development of the Atmospheric Emitted Radiance Interferometer (AERI), an instrument developed at the Space Science and Engineering Center (SSEC) at the University of Wisconsin-Madison for the Department of Energy ARM Program, and of the airborne High-Resolution Interferometer Sounder (HIS), which has been flown on the National Aeronautics and Space Administration (NASA) ER-2 research aircraft (Revercomb et al., 1988).

The M-AERI system consists of two main components: an external unit that is mounted on the deck of the ship and an electronics rack that is installed inside the vessel, the two being linked by an umbilical cable up to 60 m in length. The external unit comprises the Fourier transform infrared (FTIR) interferometer assembly (Griffiths and de Haseth, 1986) with detectors, a detector cooler, an optics chamber, calibration cavities, a scan mirror and motor, and ancillary sensors. The rack of electronics includes the computer for instrument control and data acquisition, processing and display, the interfaces and control units for the scan mirror, blackbodies, the detector cooler, and power conditioning units. A global positioning system (GPS) antenna is mounted externally. The FTIR spectrometer operates in the range of infrared wavelengths from ~3 to ~18 μm and measures spectra with a resolution of 0.5 cm^{-1}. This spectral range includes the intervals where satellite-borne infrared radiometers measure the SST in the so-called atmospheric windows where the transmission is high. The M-AERI uses two infrared detectors to achieve this wide spectral range, and these are cooled to ~78 K (i.e., close to the boiling point of

Figure1. The M-AERI installed on the foredeck of NCGC *Pierre Radisson* in the Beaufort Sea, October 2002.

* *Corresponding author address:* Peter J Minnett, Meteorology & Physical Oceanography, Rosenstiel School of Marine & Atmospheric Science, University of Miami, FL 33149-1098;
email: pminnett@rsmas.miami.edu

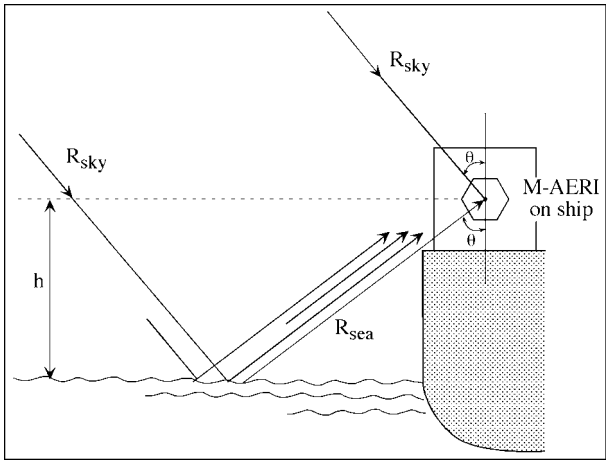

Figure 2. The M-AERI measurement geometry for the retrieval of skin SST..

liquid nitrogen) by a Stirling cycle mechanical cooler to reduce the noise equivalent temperature difference to levels well below 0.1 K. The M-AERI includes two internal blackbody cavities for accurate real-time calibration. The scan mirror is programmed to step through a preselected range of angles, directing the field of view of the interferometer to either of the blackbody calibration targets or to the environment from nadir to zenith. The interferometer integrates measurements over a preselected time interval, usually a few tens of seconds, to obtain a satisfactory signal-to-noise ratio. A typical operational cycle, including 2 view angles to the atmosphere, 1 to the ocean, and 2 calibration measurements, takes about 12 minutes.

The M-AERIs are installed on ships in a position that provides a clear view of the sea surface ahead of the bow wave, so that the measured infrared emission from the sea surface is uncontaminated by the presence of the ship. A clear view of the atmosphere, including to zenith is also required. Figure 1 shows an M-AERI installed on the foredeck of NCGC *Pierre Radisson* in the Beaufort Sea, October 2002, and Figure 2 is a cartoon of the measurement geometry.

Examples of M-AERI spectra measured from the NCGC *Pierre Radisson* in the Beaufort Sea are shown in Figure 3. Emission lines of the gaseous atmospheric

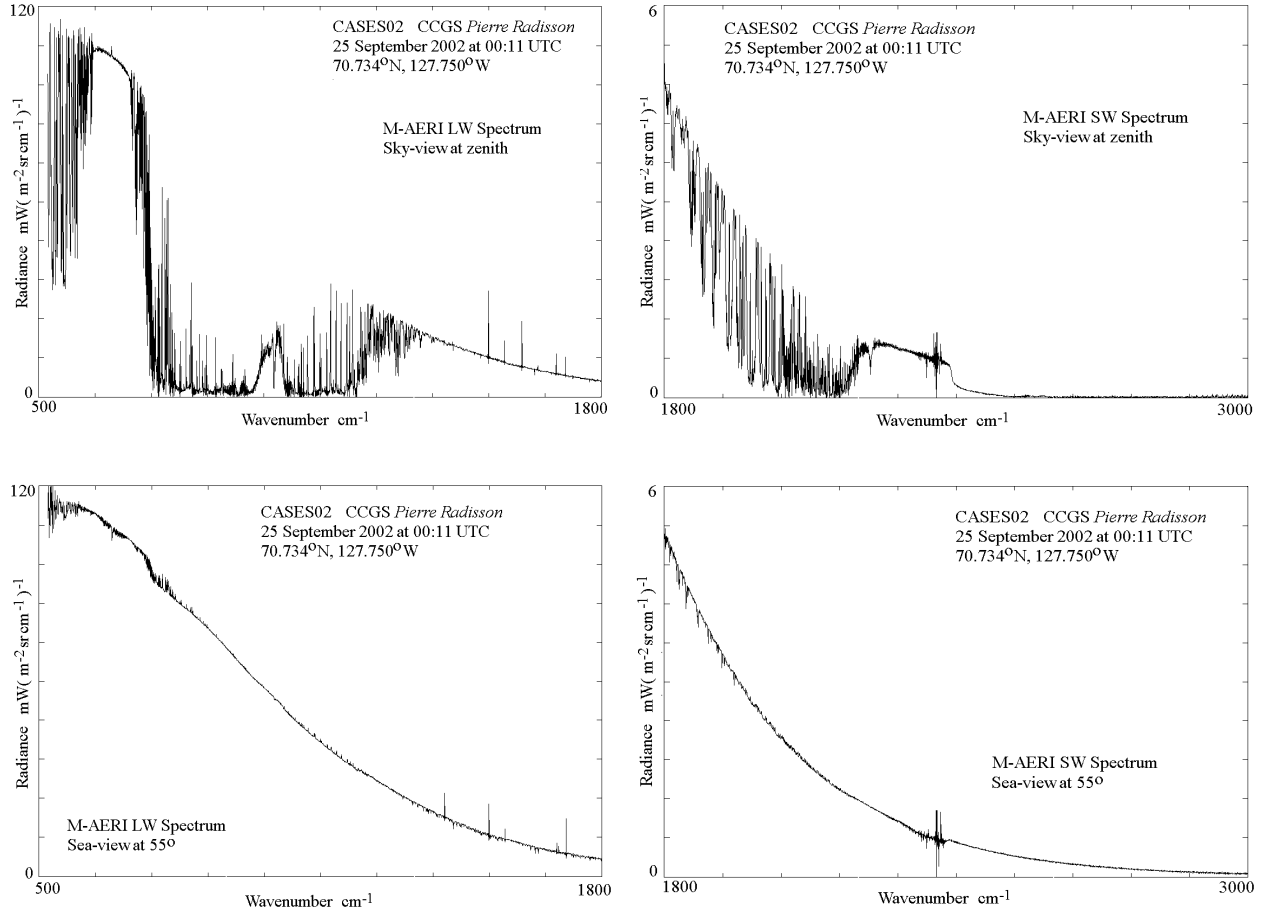

Figure 3. Examples of M-AERI spectra measured in the Arctic, from the NCGC *Pierre Radisson*, of the infrared radiation emitted from a cloud-free sky at zenith (top) and from ice-free ocean surface (below). Note the change in vertical scale between the left and right panels.

constituents cause the spikes in the atmospheric spectra.

2.1 Skin sea-surface temperature measurement

If the sea surface were a perfect blackbody, the water view would be a smooth line at the skin temperature, but the small departure from unity in the emissivity of the sea surface results in reflection of the sky radiance in the sea-viewing measurement, including the atmospheric emission lines. The retrieval of SST from these spectra requires the correction of the reflected radiance. The signal measured wavelength λ at a nadir angle θ in the downward view is:

$$R_{\text{water}}(\lambda, \theta) = \varepsilon(\lambda, \theta)B(\lambda, T_{\text{skin}}) + (1 - \varepsilon(\lambda, \theta))R_{\text{sky}}(\lambda, \theta) + R_h(\lambda, \theta)$$

where ε is the surface emissivity; and B(λ,T) is Plank's Function. R_{water}, R_{sky} and R_h are emission from the sea surface, the atmosphere above the instrument, and the atmosphere between the M-AERI and the sea-surface. Rearranging the terms gives the expression for the derivation of the skin sea-surface temperature:

$$T_{\text{skin}} = B^{-1}\langle\{R_{\text{water}}(\lambda, \theta) - [1 - \varepsilon(\lambda, \theta)]R_{\text{sky}}(\lambda, \theta) - R_h(\lambda, \theta)\}/\varepsilon(\lambda, \theta)\rangle$$

R_{water} and R_{sky} are measured, and R_h is expressed as a parameterization, determined by radiative transfer simulations, in terms of near-surface temperature and humidity, measured by conventional sensors attached to the M-AERI (Smith et al., 1996; Minnett et al., 2001). The emissivity can be derived from the M-AERI spectral measurements themselves (Wu and Smith, 1997; Hanafin and Minnett, 2004).

If the surface in the field of view is frozen, then the skin temperature retrieved is that of snow or ice. A video camera is deployed with the M-AERI in polar expeditions to provide information about surface type.

2.2 Air temperature measurements

In those parts of the infrared spectra where the atmospheric path lengths are short (but not too short so that the radiance from the blackbodies does not reach the detectors, leading to calibration problems at these wavelengths), measurements are characteristic of the atmosphere close to the instrument. Air temperature is retrieved from M-AERI spectra in the wavelength range of 14.5–14.9 μm (670–690 cm^{-1}). The temperature is characteristic of a distance of a few meters from the M-AERI aperture (Minnett et al., 2001; Minnett et al., 2004).

The validation of the M-AERI radiometric measurements of air-temperatures is problematic in that it inevitably involves comparisons with conventional measurements, which are believed to be inaccurate in certain circumstances, especially during the daytime under conditions of high insolation (Kent et al., 1993; Minnett, 2004). Comparisons at night and under high winds when, it is hoped, the conventional measurements are likely to be correct, show discrepancies of a few tenths of a degree (Minnett et al., 2001; Minnett et al., 2004). During the day, when insolation is high and winds are low, the discrepancies between the two types of measurements are then an indication of the corruption of the conventional measurements by extraneous effects. Our confidence in the absolute accuracy of the M-AERI measurements is based not only on laboratory measurements but also on comparisons in the field with independently calibrated precision radiometers (Barton et al., 2004) and tractability to NIST standards through well-characterized water-bath laboratory calibration standards (Rice et al., 2004).

2.3 Air-surface temperature difference

Given that both surface temperature and near-surface air temperature can both be derived from the spectra measured by the M-AERI, then a very accurate measurement of the air-sea, or air-ice, temperature difference can be made. Since both are measured at the same time, by the same instrument, the temperature difference should be very accurate indeed, as small residual bias errors in the calibration of the M-AERI spectra would cancel, at least to first order. This overcomes a major source of uncertainty in the conventional measurement of air-sea and air-ice temperature difference that arises from measuring a small temperature difference using two thermometers in two fluids, the thermal capacities of which differ by several orders of magnitude. Furthermore, the air temperature is measured at some distance away from the ship, thereby reducing any heat island contamination, and the surface temperature is a skin temperature, which is the temperature of the surface in contact with the atmosphere, whereas the conventional SST measurement is a bulk value that can introduce significant errors into the measurement through the contributions of near surface temperature variability in the water (Kearns et al., 2000; Minnett, 2003; Ward and Minnett, 2005). In the case of polar applications, the measurement of the air-surface temperature difference from ice-breaking research vessels can be done when the surface is freezing or melting, and therefore unsuited to supporting conventional sensors.

Figure 4 shows the air-surface temperature difference measured by an M-AERI on the NCGC *Pierre Radisson* in the Amundsen Gulf in September and October 2002. At the start of this period, the melt season was coming to an end, and the ice was soft and fragmented; there was much open water. Towards the end of this period, the open water was beginning to freeze, and grease and frazil ice types were much in evidence, as was nilas. None of these would permit conventional measurements of the surface temperature, nor the near-surface air temperature, nor the air-surface temperature difference. The same data are shown in Figure 5 as a scatter diagram, with the air-surface temperature difference plotted as a function of the

surface skin temperature. The colors indicate the date of the measurement. The vertical dashed line marks the freezing temperature for sea water (salinity = 35). The largest surface – air temperature differences occur over open water, and represent off-ice airflow (Minnett, 2003).

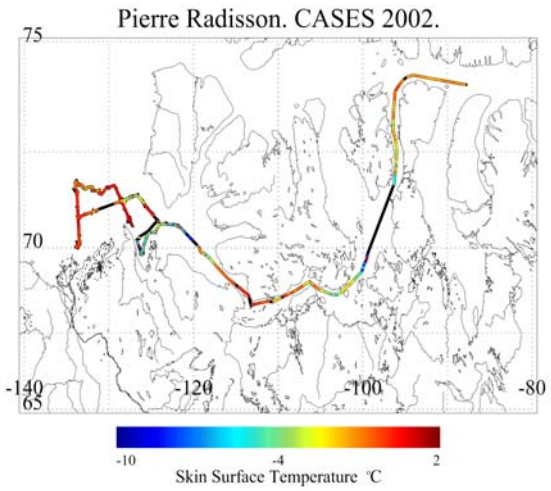

Figure 4. Air-surface temperature difference measured by an M-AERI on the NCGC *Pierre Radisson* in the Amundsen Gulf in September and October 2002. The track is that of the ship, with measurements beginning in the west, and finishing towards the eastern end of the Northwest Passage.

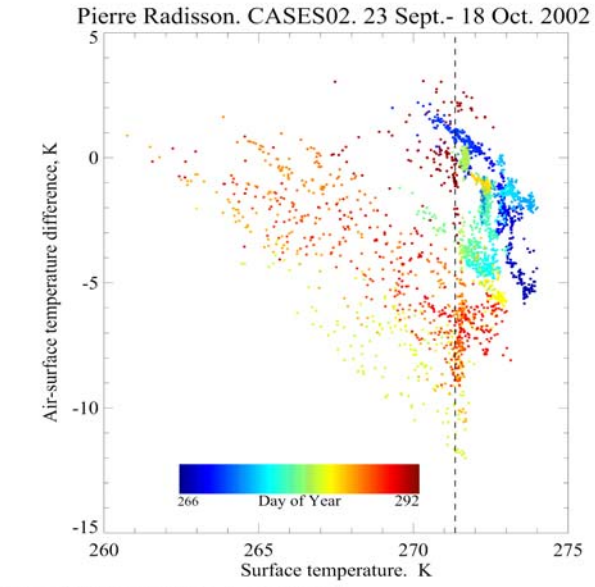

Figure 5. Scatter diagram of the air-surface temperature difference measured by the M-AERI on the NCGC Pierre Radisson (See Figure 4), as a function of the surface skin temperature. The vertical dashed line marks the freezing temperature for sea water (salinity = 35).

2.4 Atmospheric profiles of temperature and humidity

M-AERI spectra contain information about the vertical distribution of the temperature and the water vapor in the lower troposphere. This information is available in each measurement cycle (~10 minutes). The method of inverting M-AERI spectra to retrieve the profiles of temperature and water vapor in the lowest 3 km of the atmosphere is described in Smith et al., 1999 and is routinely used with the land based model of the interferometer (AERI) to retrieve the lower troposphere structure at number of ARM's sites (Feltz et al., 2003). The retrieval process of an iterative technique that requires an initial guess of the temperature and moisture profiles. In the case of M-AERI, actual profiles from radiosondes launched on board of the ship or numerical model (NCEP – National Centers for Environmental Prediction or ECMWF – European Centre for Medium-range Weather Forecasts) generated profiles are used as the first guess (Szczodrak and Minnett, 2005).
An example of profiles of atmospheric temperature and humidity profiles are shown in Figure 6 and as a time series along a ship's track in Figure 7. These data were taken in the Caribbean Sea from the *Explorer of the Seas* (Williams et al., 2002; see also http://www.rsmas.miami.edu/rccl/), but the same techniques can be applied in polar regions. The red lines on Figure 7 mark the launch times of radiosondes, released from the ship and indicate the normal sampling available from ships.

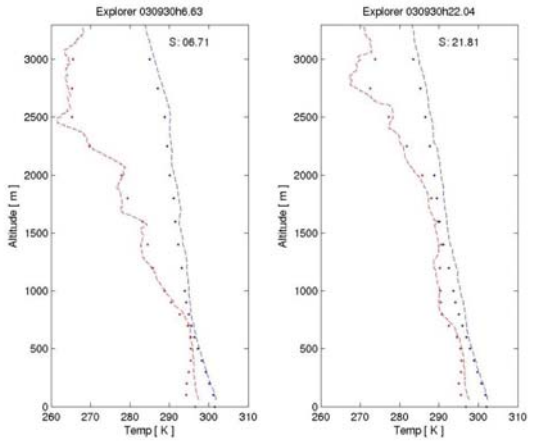

Figure 6. Profiles of atmospheric temperature and humidity measured by a radiosonde (dashed line, and the M-AER (dots). The data were taken in the Caribbean at 06:63 UTC on 30 September, 2003.

2.5 Precipitable water

Even though the profiles retrieved from the M-AERI spectra can only extend to ~3km height, this generally encompasses most of the atmospheric water vapor, and captures most of the variability. Adding the profiles from Numerical Weather Prediction models above the M-

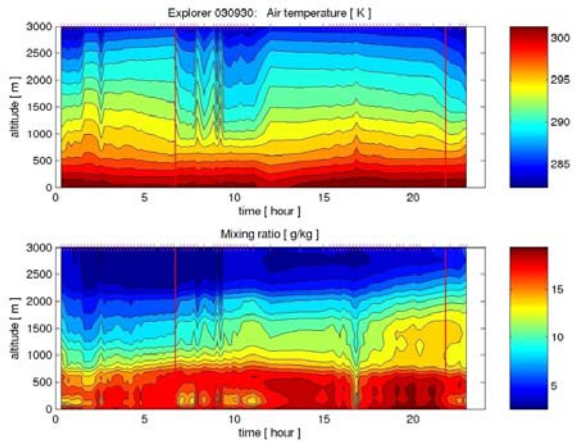

Figure 7. Sections of atmospheric temperature (top) and humidity (mixing ratio, bottom) derived from M-AERI spectra measured from the Explorer of the Seas on 30 September, 2003, in the Caribbean. Times are UTC. The two red vertical lines mark the launch times of radiosondes, released from the ship.

AERI retrievals and summation of the water vapor content can lead to a useful estimate of the precipitable water.

Figure 8 displays a time series of measurements of precipitable water above the Explorer of the Seas in the Caribbean on 30 September, 2003. Several techniques were used. The dots are the integral of water vapor measured by radiosondes, with the plus signs indicating the values when the integration is truncated at a height of 3km. The yellow line indicates the high resolution measurements from a Radiometrics WVR-1100 microwave radiometer, also installed on the ship, and the overlying dark line is a smoothed version of these data, subsampled to the times of the M-AER measurements. The lowest line is the integral to 3km height of the water vapor profile retrieved from the M-

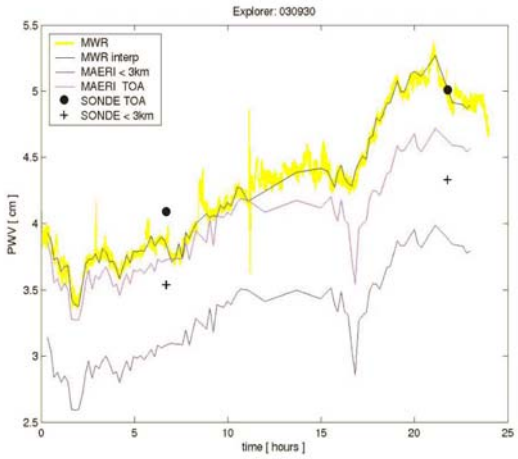

Figure 8. Time series of measurements of precipitable water above the Explorer of the Seas in the Caribbean on 30 September, 2003.

AERI spectra, and the line above is derived by extending the M-AERI profiles to the top of the atmosphere using NCEP NWP water vapor fields. The M-AERI – NWP water vapor agrees well with the microwave measurements, especially during the first part of the day. Understanding why the correspondence degraded later in the day is the subject of continuing research. However, it is noteworthy that the discrepancies between the two remote-sensing methods is no larger than between the microwave measurements, which are generally accepted as reliable and accurate determinations, and the conventional approach of using radiosondes.

2.6 Aerosol infrared radiative forcing

The radiative effects of aerosols in the climate system are generally expressed in terms of the shortwave forcing, or through modifying the albedo and longevity of clouds that are modified by the presence of aerosols. The net effect of aerosols in the shortwave part of the spectrum is to cool the surface. However, the effects in the infrared are to warm the surface, as the presence of aerosols is to reduce the optical path of the infrared spectral windows and thereby introduce a "greenhouse" effect into the atmosphere. The consequences of atmospheric aerosols in the infrared were recently quantified by comparing the measurements from the M-AERI of downwelling infrared radiation at the sea surface with modeled spectra derived using measurements of atmospheric state, but excluding the

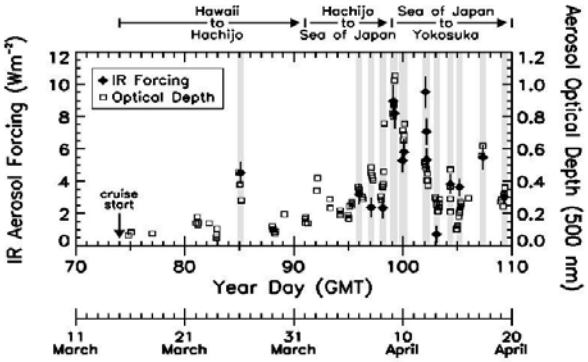

Figure 9. Observationally determined aerosol infrared forcing for the ACE Asia Experiment. The left axis gives the (daytime) aerosol infrared surface forcing (closed diamonds); the right axis gives the aerosol optical depth at 500 nm wavelength (open squares). Shading indicates days for which the aerosol infrared forcing is evaluated, which is where optical depths are greater than about 0.3 and a converged M-AERI retrieval exists. Error bars for the aerosol IR forcing are based on the analysis described in the text. Uncertainties in the optical depths are about 0.01. Cruise transit locations given above the plot. Hachijo Island is off the southeast coast of Japan; the Port of Yokosuka is located at the entrance to Tokyo Bay. From Vogelmann et al, 2003.

aerosols. The M-AERI spectra were measured on the NOAA Ship *Ronald H. Brown* during the Aerosol Characterization Experiment-Asia (ACE-Asia) in March-April 2002. The daytime surface infrared forcing was found to be a few Wm^{-2}, reaching almost 10 Wm^{-2} for large aerosol loadings (Vogelmann et al., 2003). Thus, even the smaller aerosol infrared forcing observed are comparable to or greater than the 1 to 2 Wm^{-2} infrared surface radiation enhancement from increases in greenhouse gases. These results highlight the importance of aerosol infrared forcing which should be included in climate model simulations.

This approach could also be applied to Arctic studies where the role of aerosols on the surface radiation budget is expected to be significant, but which is poorly quantified (Key, 2004).

3 SUMMARY

The M-AERIs have been deployed several times on icebreaking research vessels in polar regions. They have been shown to be robust and reliable instruments capable of providing well-calibrated measurements of the spectra of infrared emission from the surface and the polar atmosphere. A wide orange of geophysical variables of relevance to climate research can be derived from these spectra. They provide a mechanism for obtaining quantified estimates of many variables that are inaccessible by conventional means. Although not discussed here, the M-AERI measurements are also of value in the validation of satellite measurements.

The routine deployment of the M-AERI on research icebreakers also includes the use of a range of ancillary sensors, such as weather stations, all-sky cameras, radiosonde systems etc, and this ensemble of instruments, centered on M-AERIs can make an important contribution to the activities of the International Polar Year.

4 ACKNOWLEGDEMENTS

The captains, officers and crews of the various research vessels that have hosted the M-AERI and ancillary sensors are thanked for their support at sea. NASA funded the development of the M–AERIs and also contributed to the cruises during which the measurements presented here were taken.

REFERENCES

Barton, I. J., P. J. Minnett, C. J. Donlon, S. J. Hook, A. T. Jessup, K. A. Maillet, and T. J. Nightingale, 2004: The Miami2001 infrared radiometer calibration and inter-comparison: 2. Ship comparisons. *Journal of Atmospheric and Oceanic Technology*, **21,** 268-283.

Feltz, W. F., W. L. Smith, H. B. Howell, R. O. Knuteson, H. Woolf, and H. E. Revercomb, 2003: Near continuous profiling of temperature, moisture, and atmospheric stability using the atmospheric emitted radiance interferometer (AERI). *Journal of Applied Meteorology*, **42,** 584-597.

Griffiths, P. R. and J. A. de Haseth, 1986: *Fourier Transform Infrared Spectrometry*. Vol. 83, *Chemical Analysis*, John Wiley & Sons.

Hanafin, J. A. and P. J. Minnett, 2004: Measurements of the infrared emissivity of a wind-roughened sea surface. *Applied Optics.*, **Accepted**.

Kearns, E. J., J. A. Hanafin, R. H. Evans, P. J. Minnett, and O. B. Brown, 2000: An independent assessment of Pathfinder AVHRR sea surface temperature accuracy using the Marine-Atmosphere Emitted Radiance Interferometer (M-AERI). *Bulletin of the American Meteorological Society*, **81,** 1525-1536.

Kent, E. C., R. J. Tiddy, and P.K.Taylor, 1993: Correction of marine air temperature observations for solar radiation effects. *Journal of Atmospheric and Oceanic Technology*, **10,** 900-906.

Key, E. L., 2004: Cloud Radiative Forcing in Arctic Polynyas: Climatology, Parameterization and Modeling, PhD Thesis. Meteorology and Physical Oceanography. University of Miami.

Minnett, P. J., 2003: Radiometric measurements of the sea-surface skin temperature - the competing roles of the diurnal thermocline and the cool skin. *International Journal of Remote Sensing*, **24,** 5033-5047.

Minnett, P. J., 2003: Radiometric measurements of air-sea and air-ice temperature differences in the Arctic. *IEEE International Geoscience and Remote Sensing Symposium (IGARSS'03)*, Toulouse, France.

Minnett, P. J., 2004: Diurnal Signals in Air-sea Temperature Signals -- True or False? *AGU Ocean Sciences*, Portland, Oregon, USA.

Minnett, P. J., K. A. Maillet, J. A. Hanafin, and B. J. Osborne, 2004: Infrared interferometric measurements of the near surface air temperature over the oceans. *J. Atm. Ocean. Tech*, **In review.**

Minnett, P. J., R. O. Knuteson, F. A. Best, B. J. Osborne, J. A. Hanafin, and O. B. Brown, 2001: The Marine-Atmospheric Emitted Radiance Interferometer (M-AERI), a high-accuracy, sea-going infrared spectroradiometer. *Journal of Atmospheric and Oceanic Technology*, **18,** 994-1013.

Revercomb, H. E., H. Buijs, H. B. Howell, D. D. LaPorte, W. L. Smith, and L. A. Sromovsky, 1988: Radiometric calibration of IR Fourier transform spectrometers: Solution to a problem with the High Resolution Interferometer Sounder. *Applied Optics*, **27,** 3210-3218.

Rice, J. P., J. J. Butler, B. C. Johnson, P. J. Minnett, K. A. Maillet, T. J. Nightingale, S. J. Hook, A. Abtahi, C. J. Donlon, and I. J. Barton, 2004: The Miami2001 Infrared Radiometer Calibration and Intercomparison: 1. Laboratory Characterization of Blackbody Targets. *J. Atm. Ocean. Tech.*, **21,** 258-267.

Smith, W. L., W. F. Feltz, R. O. Knuteson, H. E. Revercomb, H. M. Woolf, and H.B. Howell, 1999: The retrieval if planetary boundary layer structure using ground-based infrared spectral measurements. *J. Atmosph. Oceanic Tech*, **16,** 323-333.

Smith, W. L., R. O. Knuteson, H. E. Revercomb, W. Feltz, H. B. Howell, W. P. Menzel, N. Nalli, O. Brown, J. Brown, P. Minnett, and W. McKeown, 1996:

Observations of the infrared radiative properties of the ocean - implications for the measurement of sea surface temperature via satellite remote sensing. *Bulletin of the American Meteorological Society*, **77,** 41-51.

Stamnes, K., E. R. G., J. A. Curry, J. E. Walsh, and B. D. Zak, 1999: Review of Science Issues, Deployment Strategy, and Status for the ARM North Slope of Alaska - Adjacent Arctic Ocean Climate Research Site. *J. Climate*, **12,** 46-63.

Stokes, G. M. and S. E. Schwartz, 1994: The Atmospheric Radiation Measurement (ARM) Program: Programmatic Background and Design of the Cloud and Radiation Test Bed. *Bull. Am. Met. Soc.*, **75,** 1201-1221.

Szczodrak, M. and P. J. Minnett, 2005: Profiling of the Atmospheric Boundary Layer at sea with the Marine - Atmospheric Emitted Radiance Interferometer during the Aerosol and Ocean Science Expedition. *In preparation*.

Vogelmann, A. M., P. J. Flatau, M.Szczodrak, K. Markowicz, and P. J. Minnett., 2003: Observations of Large Aerosol Infrared Forcing at the Surface. *Geophys. Res. Let.*, **30,** 1655.

Walden, V. P., M. S. Town, and B. Halter, 2005: Measurement capabilities of the Polar Atmospheric Emitted Radiance Interferometer (PAERI). *8th Conference on Polar Meteorology and Oceanography*, San Diego, CA, American Meteorology Society.

Ward, B. and P. J. Minnett, 2005: Measurements of Near Surface Temperature. *Journal of Geophysical Research*, In review.

Williams, E., E. Prager, and D. Wilson, 2002: Research Combines with Public Outreach on a Cruise Ship. *EOS*, **83,** 590, 596.

Wu, X. and W. L. Smith, 1997: Emissivity of rough sea surface for 8-13 um: modeling and verification. *Applied Optics*, **36,** 2609-2619.